Available online at www.sciencedirect.com
ScienceDirect
Ceramics International 35 (2009) 1139–1144
CERAMICS INTERNATIONAL
www.elsevier.com/locate/ceramint

Simultaneous synthesis and single-step sintering of lead magnesium niobate ceramic using mixed nanopowders

A.M. Bazargan, M. Naghavi, Mehdi Mazaheri *, S.K. Sadrnezhaad

Materials and Energy Research Center, P.O. Box: 14155-4777, Tehran, Iran

Received 1 February 2008; received in revised form 15 March 2008; accepted 20 May 2008
Available online 19 July 2008

Abstract

A high density single-phase lead magnesium niobate ceramic with the highest peak dielectric constant reported so far, has been synthesized and sintered simultaneously via a modified mixed oxide route, using mixed oxide nanopowder and single-step sintering. The mixed nanopowder was sintered at 1200 °C in air and PbO atmospheres. By comparison, samples sintered in air, gained pyrochlore structure, while those samples sintered in PbO atmosphere had pure perovskite structure. Pellets sintered for 2.5 h exhibited best dielectric properties with peak dielectric constant of 18,672 at the frequency of 1 kHz at −13 °C. The dielectric properties, compressibility, phase formation, densification, and microstructure of the samples were investigated.

Keywords: Lead magnesium niobate; Mixed oxide; Pyrochlore; Dielectric constant

1. Introduction

Lead magnesium niobate, $Pb^{2+}Mg_{1/3}{}^{2+}Nb_{2/3}{}^{5+}O_3{}^{2-}$ (PMN), is one of the most widely investigated relaxor ferroelectric materials with a perovskite structure. Globally, there is a balance of positive/negative charges. But in this system, any particular unit cell has either Mg^{2+} or Nb^{5+} at its body-centre. There is thus a local deviation from the value +4 required for charge balance. This factor is responsible for the occurrence of relaxor behavior, leading to a ''Curie range'' of temperatures, rather than a single temperature for the occurrence of the ferroelectric transition [1]. The excellent relative permittivity of PMN (∼20,000) over the operational temperature range, electrostrictive properties and low dielectric loss make it a promising electroceramic material for multilayer ceramic capacitors (MLCCs), sensors, electromechanical transducers, electro-optic applications, electrostrictive actuators and fuel injectors for automobile engines [2–5]. There has been a great deal of interest in the preparation of single-phase PMN powders as well as in the sintering and dielectric properties of PMN-based ceramics [6].

The mixed oxide synthetic route is probably one of the most fundamental, practical routine methods used in production of PMN, and it has been developed and modified in both scientific research and industrial mass production for many years [6–10]. This technique involves powder preparation (mixing, milling, drying, sieving and calcination), the forming of green bodies and densification, where heat is applied, either with pressure (HIP) or pressureless sintering [11,12]. Although many alternative *powder synthetic routes* such as co-precipitation [13], molten salt [14], sol–gel [15] as well as hydrothermal methods [16] have been introduced from time to time, widespread efforts have still been made on the modification and development of conventional mixed oxide methods.

In general, the overriding aim of any materials processing technique is to achieve a final product with consistent properties. In practice, the level of consistency obtained is often a matter of compromise, it being largely a consequence of the economics of fabrication and characterization.

The main problem in fabrication of pure perovskite PMN ceramics is formation of the unwanted pyrochlore phase with low dielectric constant (∼200) which decreases the dielectric and electromechanical performances of the resulting material [17]. The pyrochlore phase is the major product at the initial

* Corresponding author. Tel.: +98 912 169 1309; fax: +98 21 88773352.
E-mail addresses: mmazaheri@gmail.com, mazaheri@merc.ac.ir (M. Mazaheri).

0272-8842/$34.00
doi:10.1016/j.ceramint.2008.05.010

stages of the solid-state reactions between the three constituent oxides, owing to the preferential reaction between Nb_2O_5, a large amount of PbO and a small amount of MgO. With the increasing reaction temperature and time, pyrochlore further combines with the remaining PbO and MgO to yield the perovskite PMN [18]. The residual pyrochlore phase, together with the main perovskite, is a consequence of low MgO reactivity and intrinsic inhomogeneity of the reacting mixture. Furthermore, the heat treatment at temperatures above 900 °C can lead to the formation of pyrochlore phase as a consequence of PbO loss by evaporation, if samples are not fired in a saturated PbO atmosphere [17–20].

Among all the issues reported so far [6,21–25], most attention has been focused on the powder processing stage, whereas investigations of modified sintering techniques have not been widely carried out. In the case of sintering and production of single-phase PMN ceramics, Lejeune and Boilot [21] paid attention to three sintering cycles either 1000 °C for 6 h or heating to 800/830 °C followed by cooling down and heating to 1000 °C again for 6 h. The second sintering cycle (i.e. heating to 800 °C) was found to produce PMN ceramic with the best dielectric properties. Mohan and coworkers [22] prepared PMN ceramics by the semiwet hydroxide route and sintered at 1150 °C, the best dielectric constant of their samples was about 13,000 at −12 °C. Swartz et al. [23] calcined and sintered the pellets at 800 °C, 4 h and 1270 °C, 1 h, respectively, after ball-milling the oxide mixture in ethanol for 12 h and subsequent drying. The best dielectric constant was obtained ∼16,500 (1 kHz at −15 °C) with relative density of 93.35%. Wang et al. [24] used mechanochemical fabrication technique, nanosized PMN particles were formed when the oxide mixture was mechanically activated for 20 h, followed by sintering of PMN powder at 1050 °C for 1 h to reach a relative density of ∼99%. The sintered PMN exhibited K_{max} = 17,500 at a frequency of 1 kHz at −11 °C. Liou and Chen [25] produced PMN ceramic of 100% perovskite phase by simplified columbite route and then sintering at 1250 °C for 2 h. Peak dielectric constant of 17,100 at 1 kHz was obtained. Ananta and Thomas [6] utilized mixed oxide route followed by the so-called double sintering technique to achieve single-phase PMN in which the oxide mixture was calcined at 800 °C for 4 h and then sintered in two steps, first at 1025 °C, 2 h and second step at 1100 °C for 2 h. Their samples had pure provskite structure with relative density of 91% and peak dielectric constant of 14,000 at 1 kHz (−12 °C).

In the present study, an attempt has been made to fabricate full dense single-phase PMN ceramic with the best dielectric properties by employing modified mixed oxide route. High energy milling was used to reduce the size of powder down to nanoscale, followed by calcination within the single-step sintering of PMN. Compressibility, phase formation, densification, microstructure, and dielectric properties of the samples have also been investigated.

2. Experimental procedure

The modified mixed oxide route was employed for the synthesis of PMN powder. Starting raw materials were reagent-grade PbO (99%, Merck), Nb_2O_5 (99.9%, Merck) and MgO (98%, Merck). Appropriate amounts of PbO, Nb_2O_5 and MgO for stoichiometric PMN were dry-milled using a disc mill (Siebtechnik T100) with tungsten carbide discs, for 90 min at 1000 rpm. The Morphology and size of the milled powder was observed using transmission (TEM, CM200 FEG, Philips, Netherlands) and scanning (SEM, Philips XL30, Netherlands) electron microscopy. The green pellets (10 mm diameter, 3 mm thickness) were obtained by uniaxial pressing of the powder at 800 MPa in a steel cylindrical die. After ejection of compacts from die, the green density of the pellets ($64 \pm 0.5\%$ of theoretical density) was measured by water immersion method. The compressibility curve of the powder determined by pressing powder at different pressures and measuring their green densities.

Pellets were then sintered isothermally at 1200 °C up to 3 h with heating rate of 10 °C min^{-1} in closed alumina crucibles with a PbO sacrificial powder, in order for the atmosphere to be saturated with PbO. Sintering of the milled powder mixture was also performed in air for comparison. The density of sintered PMN pellets was also measured by water immersion method. Microstructures were observed by SEM. The phase formation of sintered PMN ceramics was analyzed by X-ray diffraction (XRD, PW3710-based Philips diffractometer) at 2θ between 25° and 40° with a step size of 0.02°. The relative amounts of perovskite and pyrochlore phases were determined from XRD pattern of the samples by measuring the major peak intensities for the perovskite phase ($I_{perov.}$) and pyrochlore phase ($I_{pyro.}$) related to (1 1 0) and (2 2 2), respectively. The following approximation (Eq. (1)), proposed by Swartz and Shrout [26], was used:

$$\text{perovskite}(\%) = 100 \times \frac{I_{perov.}}{I_{perov.} + I_{pyro.}} \quad (1)$$

Dielectric properties were measured by LCR meter (HP-4174 Hewlett-Packard) at 1 kHz.

3. Results and discussion

Fig. 1(a) and (b) shows the TEM micrographs of oxides mixture after milling. Size of the mixed powder was also estimated by SEM to be in the range of 50–80 nm which is in good agreement with TEM micrographs (30–70 nm). As it is seen in Fig. 1(b), milling has been done properly and the oxides are mixed perfectly, however, no PMN phase was observed in the X-ray diffraction of as-milled powder.

Fig. 2(a) demonstrates the change of green density of the samples as a function of the applied pressure. As shown in this figure, green densities increased with compaction pressure. Their increasing rate decelerated, however, with the compaction pressure until they finally reached to a nearly flat plateau (at around 800 MPa). No obvious improvement in the densification was achieved with further escalation of the pressure. A green density increase of up to 66% with respect to the theoretical value was achieved by enhancement of the applied pressure from 100 to 1100 MPa. Except 1300 MPa which resulted in

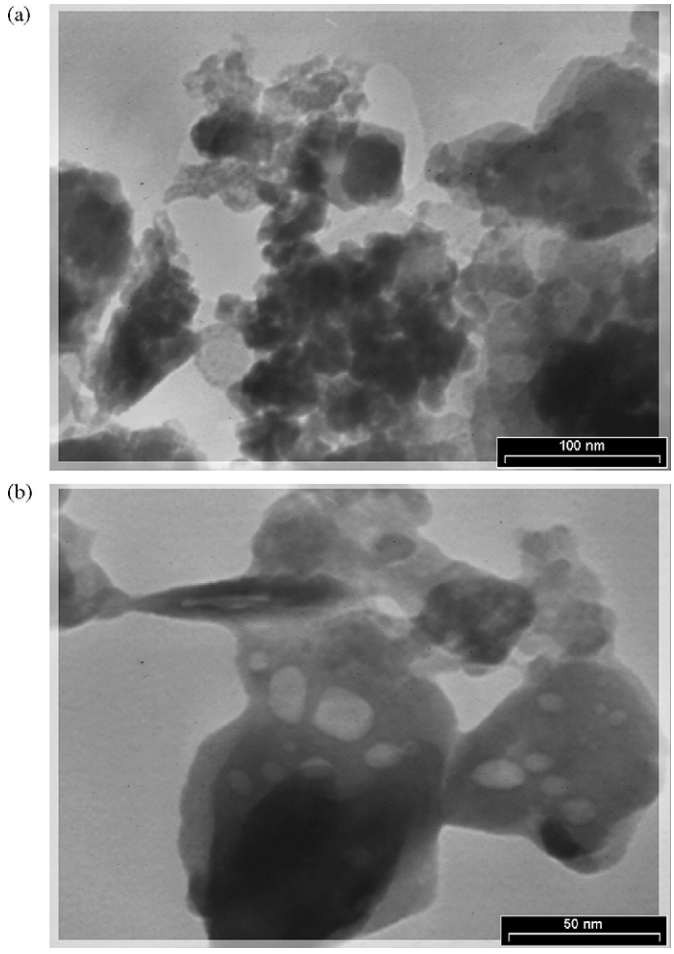

Fig. 1. TEM micrographs of oxides mixture after milling.

lamination in the samples, no lamination was generally observed at pressures applied to consolidate the milled powder in this research.

One of the most crucial features of producing fully dense ceramics is the powder compressibility, by which the compact green density and therefore the fired density are directly contributed. Applying a ceramic powder with a good potential of compression can lead to a lower sintering temperature and therefore accessing an ultrafine structure. The powder compressibility, regards to Khasanov instructions [27], is evidently influenced by key elements (P_{cr} and b) in the following equation:

$$\rho = b \ln\left(\frac{P_{pr}}{P_{cr}}\right) + 1 \quad (2)$$

where ρ is the relative density of a green compact, P_{pr} the compaction pressure and b is the constant describing densification intensity (compressibility) of compacted powder at any P_{pr} value. P_{cr} is the extrapolated value of the critical compaction pressure at which the void-free condition of a green compact is reached. The coefficients b and P_{cr} fully describe the powder compressibility, higher b accompanying with a low P_{cr} can lead to an optimum compaction circumstances. Fractional density of the powder compacts as a function of the logarithm of the

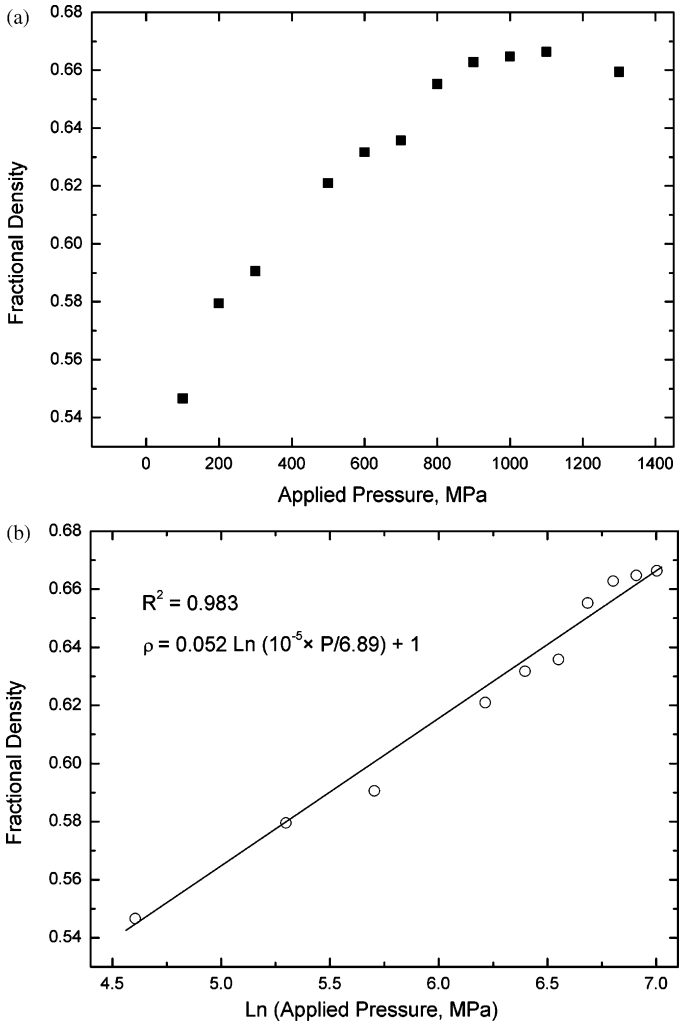

Fig. 2. (a) The effect of applied pressure on the green density of powder compacts and (b) fractional density of the powder compacts as a function of the logarithm of the applied pressure.

applied pressure is presented in Fig. 2(b). The values of coefficients b and P_{cr} have also been calculated for the milled powder to be 0.052 and 6.89×10^5 MPa, correspondingly, which depict acceptable compressibility of the powder (compared to other nanopowders in the Khasanov study) [27,28].

The relative density, average grain size, amount of perovskite phase of samples (samples no. 1–5) sintered for different soaking times and in different atmospheres, are listed in Table 1. Weight loss of PMN ceramics during sintering procedure can be thought as a measure of the degree of PbO volatilization [6,25]. This was analyzed by recording the weights of the pellets before and after sintering. By employing the PbO sacrificial powder during the sintering process, the level of weight loss can be limited to less than 5% in the system. The XRD profile of PMN ceramics sintered at 1200 °C for 2, 2.5 and 3 h in PbO atmosphere are shown in Fig. 3. The major peak (2 2 2) of pyrochlore phase at $2\theta = 29.2^\circ$ is not found in the pattern for samples no. 1 and 2. It indicates that our modified mixed oxide route is simple and effective in producing pyrochlore-free PMN ceramics. According to the thermodynamics laws, the effects of particle size (d) on the intrinsic

Table 1
Sintering behavior of mixed oxide nanopowder

Sample No.	Sintering temperature (°C)	Soaking time (h)	Density (%)	Weight loss (%)	Grain size (μm)	Perovskite phase (wt%)
1+	1200	2	97.2	0.3	0.5–3	100
2+	1200	2.5	98.5	1.7	1–5	100
3+	1200	3	98.2	2.9	2–6	98.5
4*	1200	1	97.0	5.9	–	14
5*	1200	2	96.5	7.8	–	3.5

The samples have been sintered in PbO atmosphere+ and air*.

driving force ΔE_s (superfluous surface energy) of sintering was estimated by the following equation [29]:

$$\Delta E_s = \gamma_{sv} W_m S_p = 6 \times 10^3 \frac{\gamma_{sv} W_m}{\rho_{th} d} \quad (3)$$

where γ_{sv} is the surface energy of gas–solid interface (J m^{-2}), W_m is the molecular weight (g mol^{-1}), S_p is the specific surface area (m^2 g^{-1}) and ρ_{th} is the theoretical density of the solid solution oxide (g cm^{-3}). The smaller the starting particle size, the larger the specific surface area, and subsequently the higher the driving force for densification and reactivity of starting powders. Furthermore, the low intrinsic reactivity of MgO is compensated. Thus, the time and temperature required for the calcination reaction and then sintering will decrease. Calcination reaction was carried out during heating up to soaking temperature, then sintering started and completed after 2.5 h. Hence, taking this advantage of nanopowders, synthesis and sintering of the PMN ceramics were performed simultaneously.

In Fig. 4(a) and (b), microstructure of PMN ceramics sintered in PbO atmosphere at 1200 °C for 2 and 2.5 h, respectively, confirm results of XRD patterns and no pyrochlore phase is found in these micrographs. However, the advantage of SEM here lies in its ability to reveal microstructural features often missed by X-ray diffraction, such as MgO and PbO inclusions. The average grain size was determined from the SEM images using the ImageJ software [30]. Although, our crucibles were sealed, after the 2.5 h of soaking time, the PbO atmosphere began to effuse out of the system and resulted in evaporation of PbO from the pellets, reduction of relative density of the sample (see Table 1), destabilizing the perovskite phase and formation of pyrochlore phase by the following decomposition reaction at temperatures above 900 °C [20,31]:

$$Pb_3(MgNb_2)O_9 \rightarrow Pb_{3-x}(MgNb_2)O_{9-x} + PbO(g)$$

Therefore, the major peak of pyrochlore appeared in XRD pattern of sample no. 3 (Fig. 3). Fig. 5 shows the XRD pattern of samples sintered at 1200 °C for 1 and 2 h in air. Despite some papers which have reported the fabrication of pyrochlore-free PMN ceramics by sintering stoichiometric pellets in air [32], present results obtained from Fig. 4 for samples no. 4 and 5 show formation of pyrochlore phase up to 96.5%. According to reaction mentioned above, it is impossible to prepare pyrochlore-free PMN ceramics by sintering stoichiometric pellets in air.

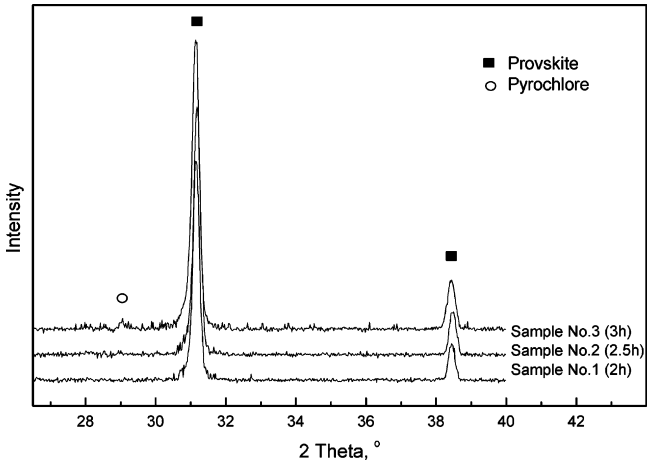

Fig. 3. The XRD pattern of PMN ceramics sintered at 1200 °C for 2, 2.5 and 3 h, in PbO atmosphere.

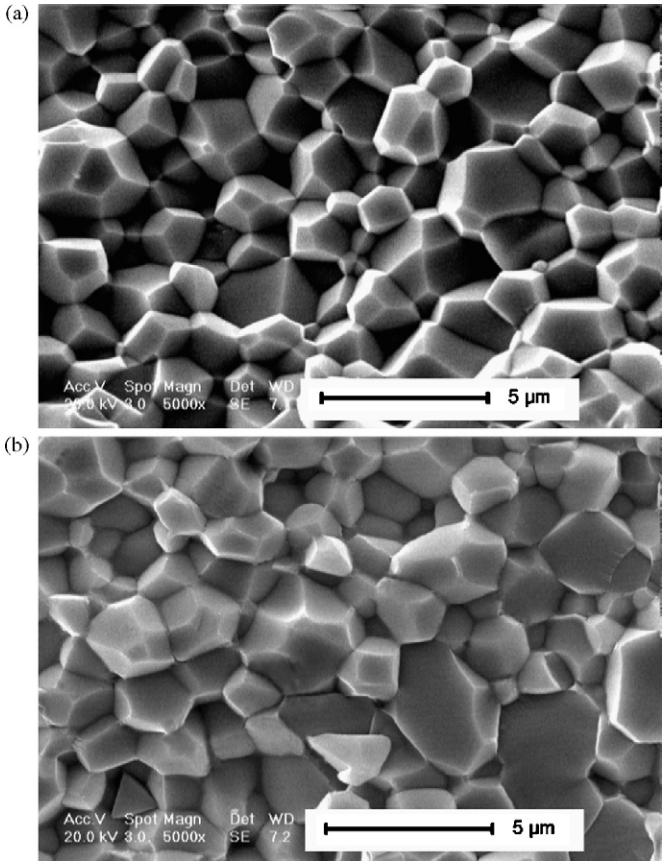

Fig. 4. SEM micrograph of PMN ceramics sintered at 1200 °C for (a) 2 h and (b) 2.5 h in PbO atmosphere.

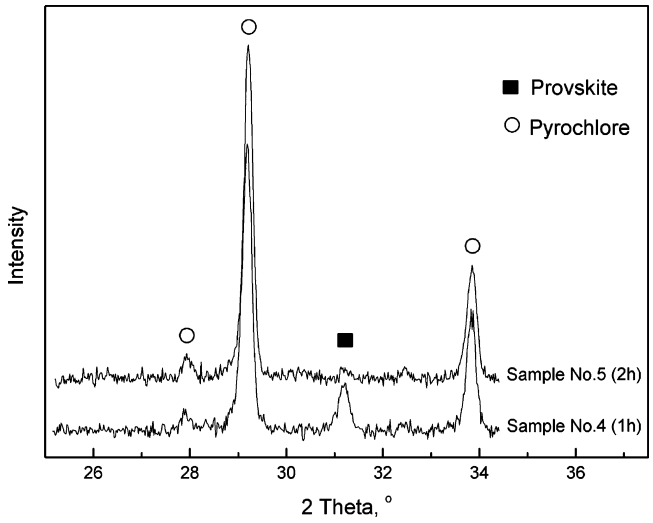

Fig. 5. The XRD pattern of samples sintered at 1200 °C for 1 and 2 h in air.

The temperature dependence of dielectric constant for samples sintered in PbO atmosphere at 1 kHz is shown in Fig. 6. The dielectric constant values were corrected for porosities by using a relation [22,23,33] $K = K_{measured} \times$ (theoretical density/sintered density), peak dielectric constants are listed in Table 2. As seen in Table 2, sample no. 2 exhibits higher maximum dielectric constant due to its pyrochlore-free structure and its larger grain size than that of sample no. 1 [11,13,22,23,34,35]. The increase in dielectric constant with grain size can be explained by the influence of low-permittivity grain boundaries. The dielectric constant in PMN ceramics is reported to depend on grain size and also on grain boundary thickness following a relation given below:

$$\frac{1}{K} = \frac{1}{K_{crystal}} + \frac{1}{RK_{GB}} \quad (4)$$

where K is the maximum dielectric constant of ceramic sample, $K_{crystal}$ is the maximum dielectric constant of PMN crystal, R is the ratio of grain size to grain thickness and K_{GB} is the dielectric constant of grain boundary phase.

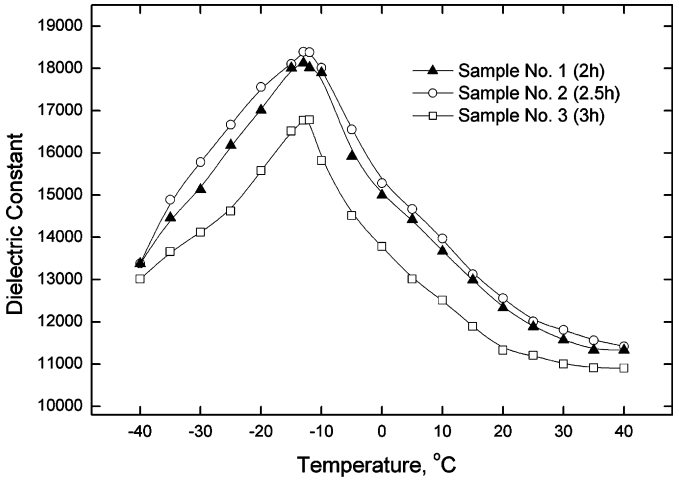

Fig. 6. The temperature dependence of dielectric constant at 1 kHz of PMN ceramics sintered at 1200 °C for 2, 2.5 and 3 h, in PbO atmosphere.

Table 2
Dielectric properties of PMN ceramics sintered at 1200 °C in PbO atmosphere

Sample no.	K_{max} (1 kHz)	T_{max} (°C)	Perov. (wt%)
1	18650	−13	100
2	18672	−13	100
3	17086	−12	98.5

It is reported that grain boundary phase is made of lead based material [33,35]. In the sample no. 3, formation of pyrochlore phase has reduced dielectric constant. Increasing the sintering time, and thus PbO loss, would change the stoichiometry of PMN and the transition temperature would be expected to decrease [23].

4. Conclusion

A high density (∼99% of theoretical density) single-phase PMN ceramic with the peak dielectric constant of 18,672 at the frequency of 1 kHz at −13 °C, has been synthesized and sintered simultaneously via a modified mixed oxide route, using mixed oxide nanopowder and single-step sintering. The results revealed that our modified mixed oxide route is effective in producing pyrochlore-free PMN ceramics. It has been proven that sintering the stoichiometric pellets in air results in the formation of pyrochlore phase. The results obtained from dielectric measurement of the samples, also indicated positive effect of grain growth on dielectric properties.

References

[1] S.M. Gupta, P. Pandit, P. Patro, A.R. Kulkarni, V.K. Wadhawan, A comparative dielectric relaxation study of PMN–PT and PMN–PZ ceramics using impedance spectroscopy, Materials Science and Engineering B 120 (1–3) (2005) 194–198.
[2] G.H. Haertling, Ferroelectric ceramics: history and technology, Journal of the American Ceramic Society 82 (4) (1999) 797–818.
[3] A.J. Moulson, J.M. Herbert, Electroceramics, Wiley, Chichester, 2003.
[4] J.F. Scott, Applications of modern ferroelectrics, Science 315 (5814) (2007) 954–959.
[5] R. Wongmaneerung, T. Sarakonsri, R. Yimnirun, S. Ananta, Effects of magnesium niobate precursor and calcination condition on phase formation and morphology of lead magnesium niobate powders, Materials Science and Engineering B 132 (3) (2006) 292–299.
[6] S. Ananta, N.W. Thomas, Fabrication of PMN and PFN ceramics by a two-stage sintering technique, Journal of the European Ceramic Society 19 (16) (1999) 2917–2930.
[7] C.M. Beck, N.W. Thomas, I. Thompson, Cobalt-doping of lead magnesium niobium titanate: chemical control of dielectric properties, Journal of the European Ceramic Society 18 (12) (1998) 1679–1684.
[8] K. Ran Han, J. Wung Jeong, C.-S. Kim, Y.-S. Kwon, Low-temperature fabrication of 0.65 PMN–0.35 PT by a mixed oxide method, Materials Letters 60 (29–30) (2006) 3596–3600.
[9] T.R. Shrout, A. Halliyal, Preparation of lead-based ferroelectric relaxor for capacitors, Journal of the American Ceramic Society 66 (1987) 704–711.
[10] J. Wang, X. Junmin, W. Dongmei, N. Weibeng, Mechanochemically synthesized lead magnesium niobate, Journal of the American Ceramic Society 82 (5) (1999) 1358–1360.

[11] N. Kim, D.A. McHenry, S.-J. Jang, T.R. Shrout, Fabrication of optically transparent lead magnesium niobate polycrystalline ceramics using hot isostatic pressing, Journal of the American Ceramic Society 73 (4) (1990) 923–928.
[12] M. Yokosuka, Electrical and electromechanical properties of hot-pressed $Pb(Fe_{1/2}Nb_{1/2})O_3$ ferroelectric ceramics, Japan Journal of Applied Physics 32 (1993) 1142–1146.
[13] A. Watanabe, H. Haneda, Y. Moriyoshi, S. Shirasaki, S. Kuramoto, H. Yamamura, Preparation of lead magnesium niobate by a coprecipitation method, Journal of Materials Science 27 (5) (1992) 1245–1249.
[14] K. Katayama, M. Abe, T. Akiba, H. Yanagida, Sintering and dielectric properties of single-phase $Pb(Mg_{1/3}Nb_{2/3})O_3$-$PbTiO_3$, Journal of the European Ceramic Society 5 (3) (1989) 183–191.
[15] W.F.A. Su, Effects of additives on perovskite formation in sol–gel derived lead magnesium niobate, Materials Chemistry and Physics 62 (1) (2000) 18–22.
[16] K. Yanagisawa, Formation of perovskite-type $Pb(Mg_{1/3}Nb_{2/3})O_3$ under hydrothermal conditions, Journal of Materials Science Letters 12 (23) (1993) 1842–1843.
[17] A.L. Costa, C. Galassi, E. Roncari, Direct synthesis of PMN samples by spray-drying, Journal of the European Ceramic Society 22 (13) (2002) 2093–2100.
[18] O. Bouquin, M. Lejeune, J.-P. Boilot, Formation of the perovskite phase in the $PbMg_{1/3}Nb_{2/3}O_3PbTiO_3$ system, Journal of the American Ceramic Society 74 (5) (1991) 1152–1156.
[19] S. Ananta, N.W. Thomas, Relationships between sintering conditions, microstructure and dielectric properties of lead iron niobate, Journal of the European Ceramic Society 19 (10) (1999) 1873–1881.
[20] Y. Narendar, G.L. Messing, Kinetic analysis of combustion synthesis of lead magnesium niobate from metal carboxylate gels, Journal of the American Ceramic Society 80 (4) (1997) 915–924.
[21] M. Lejeune, J.P. Boilot, Optimization of dielectric properties of lead-magnesium niobate ceramics, American Ceramic Society Bulletin 65 (4) (1986) 679–682.
[22] D. Mohan, R. Prasad, S. Banerjee, Dielectric properties of lead magnesium niobate and lead iron niobate prepared by the semiwet hydroxide route, Journal of the American Ceramic Society 84 (9) (2001) 2126–2128.
[23] S.L. Swartz, T.R. Shrout, W.A. Schulze, L.E. Cross, Dielectric properties of lead-magnesium niobate ceramics, Journal of the American Ceramic Society 67 (5) (1984) 311–314.
[24] J. Wang, X. Junmin, W. Dongmei, N. Weibeng, Mechanochemical fabrication of single phase PMN of perovskite structure, Solid State Ionics 124 (3–4) (1999) 271–279.
[25] Y.-C. Liou, J.-H. Chen, PMN ceramics produced by a simplified columbite route, Ceramics International 30 (1) (2004) 17–22.
[26] S.L. Swartz, T.R. Shrout, Fabrication of perovskite lead magnesium niobate, Materials Research Bulletin 17 (10) (1982) 1245.
[27] O.L. Khasanov, E.S. Dvilis, V.M. Sokolov, Compressibility of the structural and functional ceramic nanopowders, Journal of the European Ceramic Society 27 (2–3) (2007) 749–752.
[28] V.V. Srdic, M. Winterer, Comparison of nanosized zirconia synthesized by gas and liquid phase methods, Journal of the European Ceramic Society 26 (15) (2006) 3145–3151.
[29] S.J. Guo. Theory of Powder Sintering Metallurgy Industrial Press, 1998.
[30] W.S. Rasband. ImageJ. Bethesea, maryland, USA: US National institutes Of Health, 1997–2007.
[31] W.B. Ng, J. Wang, S.C. Ng, L.M. Gan, Processing and characterization of microemulsion-derived lead magnesium niobate, Journal of the American Ceramic Society 82 (3) (1999) 529–536.
[32] Y.-C. Liou, Effect of heating rate on properties of $Pb(Mg_{1/3}Nb_{2/3})O_3$ ceramics produced by the reaction-sintering process, Materials Letters 58 (6) (2004) 944–947.
[33] D. Mohan, R. Prasad, S. Banerjee, Effect of post sinter annealing on the dielectric constants of PMN and PFN, Ceramics International 27 (2) (2001) 243–246.
[34] H. Gu, W.Y. Shih, W.-H. Shih, Low-temperature, single step, reactive sintering of lead magnesium niobate using $Mg(OH)_2$-coated Nb_2O_5 powders, Journal of the American Ceramic Society 88 (6) (2005) 1435–1443.
[35] H.-C. Wang, W.A. Schulze, The role of excess magnesium oxide or lead oxide in determining the microstructure and properties of lead magnesium niobate, Journal of the American Ceramic Society 73 (4) (1990) 825–832.